Anisotropic interfacial tension and the equilibrium crystal shape of Kagomé-lattice eight-vertex model

2002 J. Phys. A: Math. Gen. 35 1517

(http://iopscience.iop.org/0305-4470/35/7/304)

INSTITUTE OF PHYSICS PUBLISHING JOURNAL OF PHYSICS A: MATHEMATICAL AND GENERAL

J. Phys. A: Math. Gen. **35** (2002) 1517–1531 PII: S0305-4470(02)24399-1

Anisotropic interfacial tension and the equilibrium crystal shape of Kagomé-lattice eight-vertex model

Masafumi Fujimoto

Department of Physics, Nara Medical University, Kashihara, Nara 634-8521, Japan

Received 9 May 2001, in final form 8 January 2002
Published 8 February 2002
Online at stacks.iop.org/JPhysA/35/1517

Abstract

We exactly calculate the anisotropic interfacial tension of the Kagomé-lattice eight-vertex model with the help of two types of square-lattice models. Each square-lattice model is inhomogeneous but still possesses a one-parameter family of commuting transfer matrices. From the anisotropic interfacial tension, the equilibrium shape of an inclusion of one ordered phase in an environment of another is obtained by applying the Wulff construction. Calculations are expressed by the use of differential forms on a Riemann surface of genus 1; and the equilibrium shape is written as an elliptic curve. We suggest the possibility of interpreting critical phenomena in terms of the moduli space of Riemann surfaces of genus 1.

PACS numbers: 05.50.+q, 02.10.-v, 02.20.-a, 02.40.-k, 61.50.Ah

1. Introduction

Baxter [1] studied the Z-invariant eight-vertex model, which contains a class of eight-vertex models on the Kagomé lattice as a special case; see also [2–4]. The Z-invariance was used to derive the exact per-site free energy of the Kagomé-lattice eight-vertex model (KEVM). He also established some equivalences between horizontal correlations of the KEVM and diagonal correlations of the square-lattice eight-vertex model.

In a previous paper [5] we considered the anisotropic correlation length of the KEVM. Extending the argument based on the Z-invariance into all directions is no easy task. We examined another approach: firstly, with the help of auxiliary vertices [6–8], we related the KEVM to an inhomogeneous system which possesses a one-parameter family of commuting transfer matrices. Secondly, we investigated an equation for commuting transfer matrices to determine their eigenvalues. Finally, from calculated eigenvalues, the correlation length of the KEVM was obtained with its full anisotropy.

It was shown that we have to distinguish two regions with respect to a parameter q: $0 < q < x^3$ and $x^3 < q < x^2$ $(0 < x < 1)$. In the region $0 < q < x^3$ the anisotropic correlation length is independent of q. Noting that the KEVM contains the

triangular/honeycomb-lattice Ising model as the $q \to x^4$ limit, we pointed out that the anisotropic correlation length for $0 < q < x^3$ is the same as that of the triangular/honeycomb-lattice Ising model. Moreover, by the use of a simple algebraic curve, we showed that the Kagomé-lattice Ising model, the diced-lattice Ising model, and the hard-hexagon model also have (essentially) the same anisotropic correlation length as the KEVM.

The analysis in [5] was motivated by the equilibrium crystal shape (ECS) problem [9–17]. The ECS is derived from the anisotropic interfacial tension via the Wulff construction [9]. In [10] the facet shape of a three-dimensional crystal was found by considering the square-lattice six-vertex model [2]; note that the facet shape corresponds to the ECS of the square-lattice six-vertex model. Akutsu and Akutsu [15] pointed out that the ECS of the square-lattice six-vertex model is identical to that of the square-lattice Ising model. The ECSs of the two models can be written as an algebraic curve; see (4.21) of [16]. The algebraic curve is expected to be a quite general one which appears as the ECSs of a wide class of lattice models possessing the fourfold rotational symmetry [16].

For any Ising model on a planar lattice, it was proved that the anisotropic correlation length is related to the anisotropic interfacial tension [11–15]. The algebraic curve obtained in the region $0 < q < x^3$ corresponds to the ECSs of the Ising models on the triangular, honeycomb, Kagomé and diced lattices [12, 14]. The arguments in [11–15], which were based on duality transformations, cannot be applied to the KEVM. In section 6 of [5], however, it was suggested that a relation similar to those in [11–15] is satisfied between the anisotropic correlation length and the anisotropic interfacial tension of the KEVM.

In this paper we calculate the anisotropic interfacial tension of the KEVM. Then we investigate a connection between the ECS of the KEVM and the algebraic curve in [5]. The outline of this paper is as follows: in section 2 we generalize the method in [5]. In section 3 we find the anisotropic interfacial tension of the KEVM. The ECS is obtained by applying the Wulff construction. Section 4 is devoted to a summary and discussion. We suggest a possibility of interpreting critical phenomena in terms of the moduli space of compact Riemann surfaces of genus 1.

2. Auxiliary vertices method

Using the method in [5] with some modifications, we find the anisotropic interfacial tension of the KEVM. In section 3 of [5] we defined an inhomogeneous system containing six spectral parameters. Here the inhomogeneous system is generalized into systems (A) and (B); each of the two systems contains eight spectral parameters. In next section the anisotropic interfacial tension is obtained from their finite-size correction terms (see also [6–8] and [16]).

Suppose a square lattice of $4N + 2N'$ columns and $2M$ rows. In the eight-vertex model an arrow is placed on every edge so that an even number of arrows point into and out of each site (or vertex) [2]. Arrow configurations are represented by associating an arrow-spin α_j with each edge j; $\alpha_j = +1$ if the corresponding arrow points up or to the right, and $\alpha_j = -1$ otherwise. Different Boltzmann weights are assigned to the different configurations around a vertex. By $W(\nu, \alpha|\beta, \mu)$ we denote the Boltzmann weight around a vertex with arrow-spins ν, α, μ and β in anticlockwise order starting from the west edge. It is convenient to parametrize the Boltzmann weights W in terms of the theta functions:

$$\begin{aligned}
a &= W(++|++) = W(--|--) = -\mathrm{i}\rho\Theta(\mathrm{i}\lambda)H[\mathrm{i}(\lambda-u)/2]\Theta[\mathrm{i}(\lambda+u)/2] \\
b &= W(+-|-+) = W(-+|+-) = -\mathrm{i}\rho\Theta(\mathrm{i}\lambda)\Theta[\mathrm{i}(\lambda-u)/2]H[\mathrm{i}(\lambda+u)/2] \\
c &= W(+-|+-) = W(-+|-+) = -\mathrm{i}\rho H(\mathrm{i}\lambda)\Theta[\mathrm{i}(\lambda-u)/2]\Theta[\mathrm{i}(\lambda+u)/2] \\
d &= W(++|--) = W(--|++) = \mathrm{i}\rho H(\mathrm{i}\lambda)H[\mathrm{i}(\lambda-u)/2]H[\mathrm{i}(\lambda+u)/2]
\end{aligned} \tag{2.1}$$

where ρ is a normalization factor, λ the crossing parameter and u the spectral parameter; for definitions of the theta functions (and related elliptic functions), see appendix A of [17] (or [16]); we denote the nome by q, the quarter-periods by I and I', and the modulus by k.

The Boltzmann weights W satisfy the Yang–Baxter relation [2, 18–20]

$$\sum_{\gamma,\mu'',\nu''} W(\mu,\alpha|\gamma,\mu''|u)W(\nu,\gamma|\beta,\nu''|u')W(\nu'',\mu''|\nu',\mu'|u'') = \sum_{\gamma,\mu'',\nu''} W(\nu,\mu|\nu'',\mu''|u'')W(\mu'',\alpha|\gamma,\mu'|u')W(\nu'',\gamma|\beta,\nu'|u) \tag{2.2}$$

for all $\alpha, \beta, \mu, \nu, \mu', \nu' = \pm 1$ with $u' = u + u'' + \lambda$. The following properties are also satisfied by W [18–20]: the standard initial condition

$$W(\nu,\alpha|\beta,\mu|-\lambda) = \rho h(\lambda)\delta(\nu,\beta)\delta(\alpha,\mu) \tag{2.3}$$

the crossing symmetry

$$W(\nu,\alpha|\beta,\mu|-u) = W(\alpha,-\mu|-\nu,\beta|u) \tag{2.4}$$

and the local inversion relation

$$\sum_{\alpha',\beta'} W(\alpha,\beta|\alpha',\beta'|-\lambda+u)W(\alpha',\beta'|\alpha'',\beta''|-\lambda-u) = \rho^2 h[(2\lambda+u)/2]h[(2\lambda-u)/2]\delta(\alpha,\alpha'')\delta(\beta,\beta'') \tag{2.5}$$

where $\delta(\cdot,\cdot)$ denotes the Kronecker symbol and $h(u)$ is defined by

$$h(u) = -\mathrm{i}\Theta(0)\Theta(\mathrm{i}u)H(\mathrm{i}u). \tag{2.6}$$

From (2.3) and (2.4) we obtain

$$W(\nu,\alpha|\beta,\mu|\lambda) = \rho h(\lambda)\delta(\nu,-\alpha)\delta(\beta,-\mu). \tag{2.3$'$}$$

Using (2.4) in (2.5) gives

$$\sum_{\alpha',\beta'} W(\beta',\beta|\alpha',\alpha|\lambda+u)W(\beta'',-\beta'|\alpha'',-\alpha'|\lambda-u) = \rho^2 h[(2\lambda+u)/2]h[(2\lambda-u)/2]\delta(\alpha,-\alpha'')\delta(\beta,-\beta''). \tag{2.5$'$}$$

We introduce two inhomogeneous systems. Assume that the spectral parameter u and the normalization factor ρ can vary from site to site. The values of u and ρ for the site (i, j) are denoted by u_{ij} and ρ_{ij}, respectively. For $0 \leqslant i \leqslant 4N-1$ set the u_{ij} to be

$$u_{ij} = \begin{cases} -\nu'' & \text{if } i \equiv 0,2 \pmod 4, \quad j \equiv 0 \pmod 2 \\ \nu & \text{if } i \equiv 1 \pmod 4, \quad j \equiv 0 \pmod 2 \\ \lambda & \text{if } i \equiv 3 \pmod 4, \quad j \equiv 0 \pmod 2 \\ -\nu' & \text{if } i \equiv 0,2 \pmod 4, \quad j \equiv 1 \pmod 2 \\ -\lambda & \text{if } i \equiv 1 \pmod 4, \quad j \equiv 1 \pmod 2 \\ -\nu & \text{if } i \equiv 3 \pmod 4, \quad j \equiv 1 \pmod 2 \end{cases} \tag{2.7}$$

(figure 1), and for $4N \leqslant i \leqslant 4N + 2N' - 1$

$$u_{ij} = \begin{cases} -\lambda + \nu' - \nu'' & \text{if } i \equiv j \equiv 0 \pmod 2 \\ -\lambda & \text{if } i + j \equiv 1 \pmod 2 \\ -\lambda - \nu' + \nu'' & \text{if } i \equiv j \equiv 1 \pmod 2 \end{cases} \tag{2.8a}$$

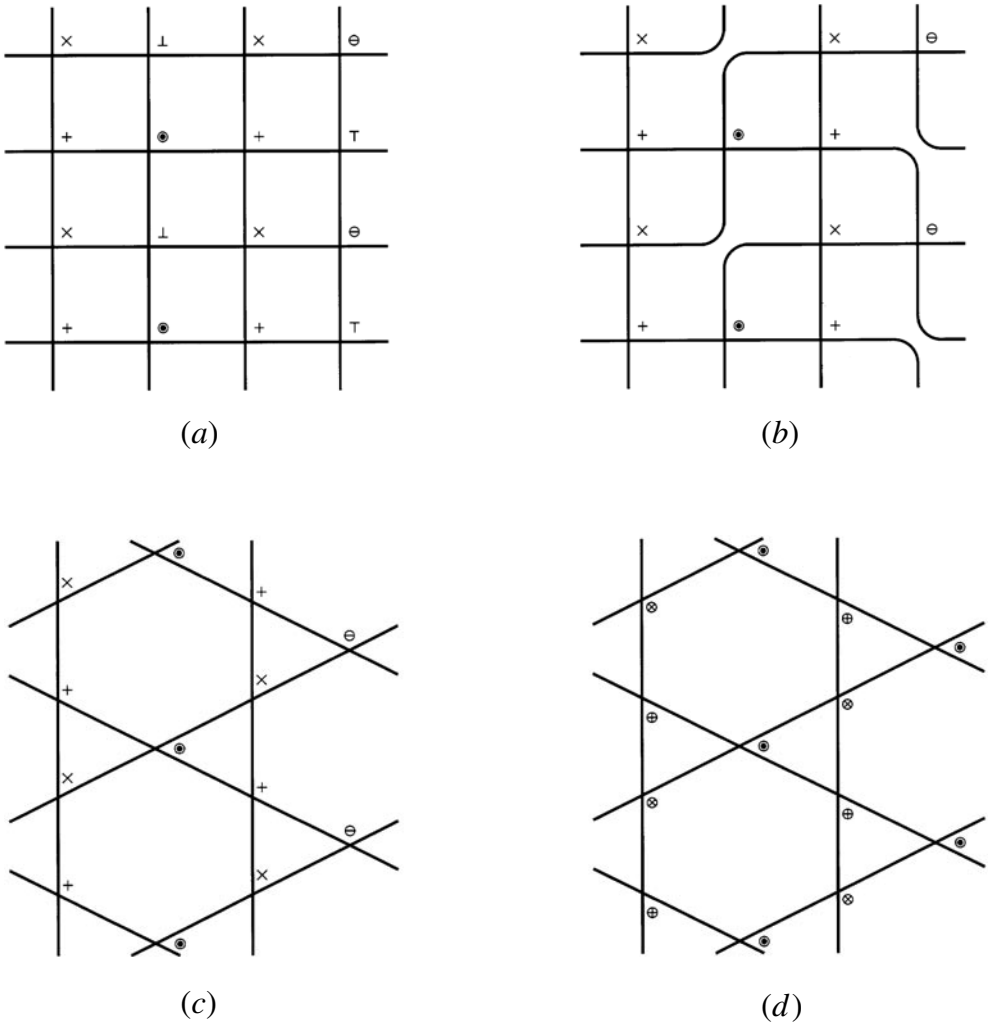

Figure 1. (*a*) For $0 \leqslant i \leqslant 4N-1$ we set u_{ij} as shown in (2.7). Vertices $u_{ij} = v$ (respectively $-v$, $-v'$, $-v''$, λ, $-\lambda$) are denoted by $\odot$ (respectively $\ominus$, $\times$, $+$, $\top$, $\perp$). (*b*) Decomposing auxiliary vertices $u_{ij} = \lambda$ and $-\lambda$, we deform the square lattice into a Kagomé lattice. (*c*) The Kagomé lattice consists of four types of vertices: $u = \pm v$, $-v'$ and $-v''$. (*d*) We use (2.4) to change the orientation of the vertices $u_{ij} = -v$ (respectively $-v'$, $-v''$) with their spectral parameter replaced by v (respectively v', v''); vertices $u_{ij} = v'$ are represented by $\otimes$, $u_{ij} = v''$ by $\oplus$.

or

$$u_{ij} = \begin{cases} \lambda & \text{if } i + j \equiv 0 \pmod 2 \\ \lambda + v' - v'' & \text{if } i \equiv 1,\ j \equiv 0 \pmod 2 \\ \lambda - v' + v'' & \text{if } i \equiv 0,\ j \equiv 1 \pmod 2 \end{cases} \tag{2.8b}$$

where

$$v' = v + v'' + \lambda \tag{2.9}$$

(figure 2). The system with (2.8*a*) (respectively (2.8*b*)) is called (A) (respectively (B)).

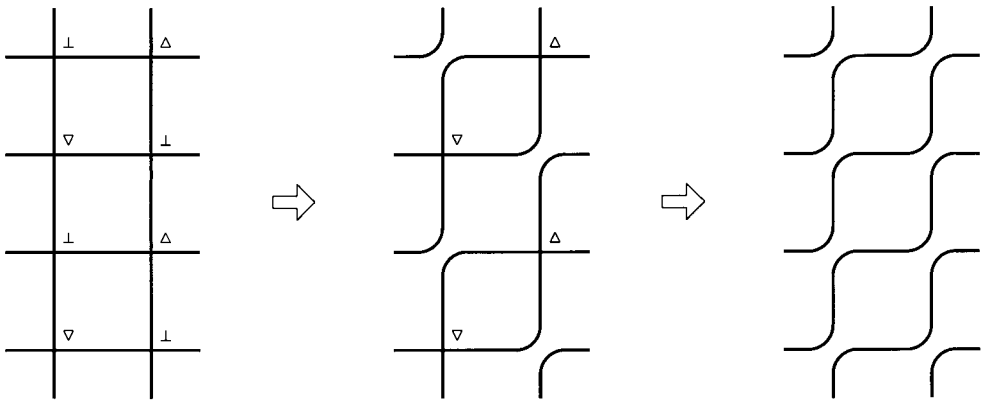

(*a*)

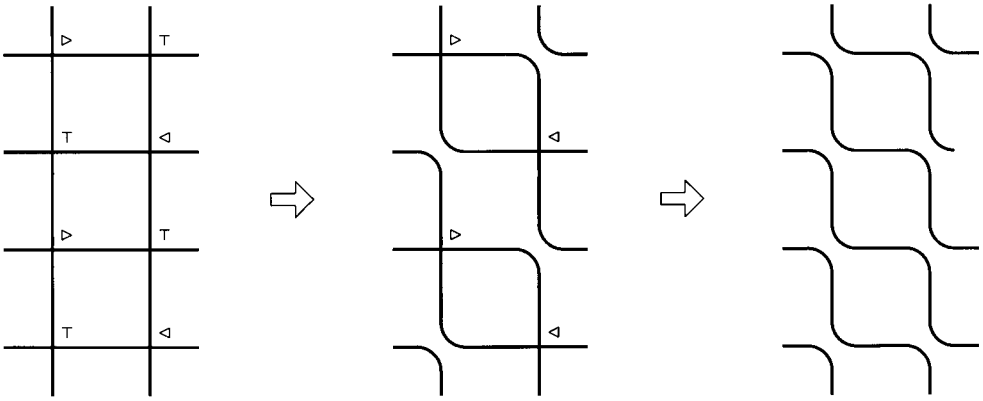

(*b*)

Figure 2. The effect of the region $4N \leqslant i \leqslant 4N + 2N' - 1$. (*a*) For the inhomogeneous system (A) we set u_{ij} as shown in (2.8*a*); vertices $u_{ij} = -\lambda$ (respectively $-\lambda + v' - v''$, $-\lambda - v' + v''$) are indicated by $\perp$ (respectively $\triangledown$, $\triangle$). (*b*) For the inhomogeneous system (B) u_{ij} are given by (2.8*b*); vertices $u_{ij} = \lambda$ (respectively $\lambda + v' - v''$, $\lambda - v' + v''$) are denoted by $\top$ (respectively $\triangleleft$, $\triangleright$). For the inhomogeneous system (A) (respectively (B)) the standard initial condition (2.3) (respectively (2.3′)) is used to decompose vertices $u_{ij} = -\lambda$ (respectively $u_{ij} = \lambda$); then, with the help of the local inversion relation (2.5) (respectively (2.5′)), we find that the region $4N \leqslant i \leqslant 4N + 2N' - 1$ corresponds to the column-to-column shift operator.

For both inhomogeneous systems (A) and (B) we set the ρ_{ij} to be

$$\rho_{ij} = \begin{cases} \rho_K & \text{if } 0 \leqslant i \leqslant 4N - 1 \\ (\rho_K \rho_S)^{1/2} & \text{if } 4N \leqslant i \leqslant 4N + 2N' - 1 \end{cases} \tag{2.10}$$

where

$$\rho_K = 1/h(\lambda) \tag{2.11a}$$

$$\rho_S = 1/\{h[(2\lambda + v' - v'')/2]h[(2\lambda - v' + v'')/2]\}^{1/2} \tag{2.11b}$$

with the function $h(u)$ defined by (2.6).

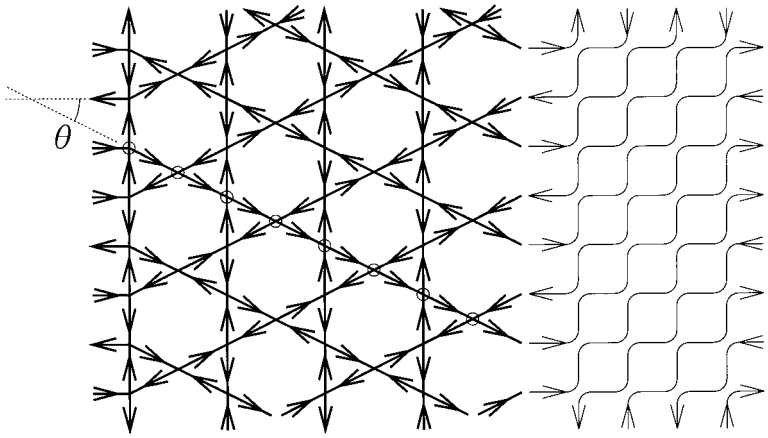

Figure 3. Typical configuration of the inhomogeneous system (A) in the zero-temperature limit. There exists an interface, which is indicated by open circles. Because of the region $4N \leqslant i \leqslant 4N + 2N' - 1$, the interface is sloped. The average slope is represented by θ, which is the angle between the horizontal axis and the line connecting the two endpoints of the interface.

The inhomogeneous systems (A) and (B) are related to the KEVM. Firstly, for $0 \leqslant i \leqslant 4N - 1$, we repeat the argument in section 3 of [5]; see also [6–8]. Vertices $u_{ij} = \pm\lambda$ are auxiliary ones (figure 1(a)). With the help of the standard initial condition (2.3), we decompose auxiliary vertices $u_{ij} = -\lambda$: the east and south edges are separated from the west and north ones at each auxiliary vertex $u_{ij} = -\lambda$. We use (2.3′) for auxiliary vertices $u_{ij} = \lambda$. They are decomposed similarly: the east and north edges are separated from the west and south ones. After all the auxiliary vertices are decomposed (figure 1(b)), we can continuously deform the square lattice into a Kagomé lattice (figure 1(c)). On the Kagomé lattice there are four types of vertices: $u_{ij} = \pm v$, $-v'$ and $-v''$. Using the crossing symmetry (2.4), we find that the region $0 \leqslant i \leqslant 4N - 1$ is equivalent to the KEVM in [5] (figure 1(d)).

Next we consider the effect of the region $4N \leqslant i \leqslant 4N + 2N' - 1$. We use the standard initial condition (2.3) (respectively (2.3′)) for vertices $u_{ij} = -\lambda$ in (A) (respectively $u_{ij} = \lambda$ in (B)); then, with the help of the local inversion relation (2.5) (respectively (2.5′)), it follows that the region $4N \leqslant i \leqslant 4N + 2N' - 1$ has the effect of shifting an arrow configuration on a column of horizontal edges along the vertical direction (figure 2).

In this paper analyses are restricted to an antiferroelectric ordered regime

$$0 < k < 1 \qquad 0 < \lambda < I' \qquad -\lambda < v < -v'' < \lambda. \tag{2.12}$$

We impose on (A) and (B) periodic boundary conditions along the horizontal direction and antiperiodic boundary conditions along the vertical direction; see section 2 of [16]. Because of the antiperiodic boundary conditions, an interface runs across the region $0 \leqslant i \leqslant 4N - 1$ (figure 3). The region $4N \leqslant i \leqslant 4N + 2N' - 1$ in (A) (respectively (B)) slope the interface by shifting the right endpoint from the left endpoint downward (respectively upward). The average slope of the interface is represented by θ, which is the angle between the horizontal axis and the line connecting the two endpoints. The ratio $\eta = N'/N$ is related to θ by

$$\text{(A)} \quad \eta = -\sqrt{3}\tan\theta \qquad -\pi/2 < \theta < 0 \tag{2.13a}$$

$$\text{(B)} \quad \eta = \sqrt{3}\tan\theta \qquad 0 < \theta < \pi/2. \tag{2.13b}$$

For the inhomogeneous systems (A) and (B), it is expected that, reflecting the existence of an interface, there is an excess free energy above the bulk free energy. We can find the anisotropic

interfacial tension of the KEVM by calculating the excess free energy as a function of η. We denote by $Z^{(1)}_{MNN'}$ the partition function of (A) (or (B)). If periodic boundary conditions are imposed in both directions, the partition function is denoted by $Z^{(0)}_{MNN'}$. The anisotropic interfacial tension σ of the KEVM is represented as

$$-\sigma/k_BT = \lim_{M,N\to\infty} \frac{\cos\theta}{2\sqrt{3}N} \ln\left[Z^{(1)}_{MNN'}/MZ^{(0)}_{MNN'}\right] \tag{2.14}$$

where the limit is taken with the ratio $\eta = N'/N$ fixed to be constant.

3. Anisotropic interfacial tension and equilibrium crystal shape

Following the program in section 2, we find the anisotropic interfacial tension of the KEVM. In section 3.1 we construct commuting transfer matrices for the inhomogeneous systems (A) and (B). In section 3.2 the partition functions in (2.14) are calculated by considering an equation for commuting transfer matrices. In section 3.3 the ECS is derived from the anisotropic interfacial tension.

3.1. Commuting transfer matrices argument

It is known that solvable systems share a common property that they have commuting transfer matrices [2, 18–20]. For the inhomogeneous systems (A) and (B), we note the constraint (2.9) to find that the spectral parameter u_{ij} can be written as $u_{ij} = v_j - w_j$ with suitable horizontal and vertical line variables v_i and w_j. Let $\bar\alpha = \{\alpha_0, \alpha_1, \ldots, \alpha_{4N+2N'-1}\}$ and $\bar\beta = \{\beta_0, \beta_1, \ldots, \beta_{4N+2N'-1}\}$ be the arrow-spins on two successive rows of vertical edges, and $\bar\mu = \{\mu_0, \mu_1, \ldots, \mu_{4N+2N'-1}\}$ the arrow-spins on a row intervening between $\bar\alpha$ and $\bar\beta$. Introducing an arbitrary horizontal line variable u, we define transfer matrices by

$$\begin{aligned}[\boldsymbol{V}(u)]_{\bar\alpha,\bar\beta} = \sum_{\bar\mu} \prod_{j=0}^{N-1} & W(\mu_{4j}, \alpha_{4j}|\beta_{4j}, \mu_{4j+1}|u) W(\mu_{4j+1}, \alpha_{4j+1}|\beta_{4j+1}, \mu_{4j+2}|u+v'-\lambda) \\ & \times W(\mu_{4j+2}, \alpha_{4j+2}|\beta_{4j+2}, \mu_{4j+3}|u) W(\mu_{4j+3}, \alpha_{4j+3}|\beta_{4j+3}, \mu_{4j+4}|u+v'-v) \\ & \times \prod_{k=0}^{N'-1} W(\mu_{4N+2k}, \alpha_{4N+2k}|\beta_{4N+2k}, \mu_{4N+2k+1}|f(u)) \\ & \times W(\mu_{4N+2k+1}, \alpha_{4N+2k+1}|\beta_{4N+2k+1}, \mu_{4N+2k+2}|g(u)) \end{aligned} \tag{3.1a}$$

where $\mu_{4N+2N'} = \mu_0$ and

$$f(u) = \begin{cases} u+v'-\lambda & \text{for (A)} \\ u+v''+\lambda & \text{for (B)} \end{cases} \qquad g(u) = \begin{cases} u+v''-\lambda & \text{for (A)} \\ u+v'+\lambda & \text{for (B).} \end{cases} \tag{3.1b}$$

The Yang–Baxter relation (2.2) shows that the transfer matrices $\boldsymbol{V}(u)$ form a one-parameter family of commuting transfer matrices.

We obtain a nonsingular matrix $\boldsymbol{Q}(u)$ which satisfies the matrix equation [2, 5, 16]

$$\boldsymbol{V}(u)\boldsymbol{Q}(u) = \phi(u-\lambda)\boldsymbol{Q}(u+2\lambda') + \phi(u+\lambda)\boldsymbol{Q}(u-2\lambda') \tag{3.2}$$

with $\lambda' = \lambda - 2\mathrm{i}I$ and

$$\begin{aligned}\phi(u) = \rho_K^{4N+N'} & \{h^2[u/2]h[(u+v'-\lambda)/2]h[(u+v'-v)/2]\}^N \\ & \times \rho_S^{N'} \{h(u+v' \mp \lambda)/2]h[(u+v''\mp\lambda)/2]\}^{N'} \end{aligned} \tag{3.3}$$

where $h(u)$ is defined by (2.6) and the upper (respectively lower) signs correspond to the inhomogeneous system (A) (respectively (B)); we use this convention throughout this section.

Since $\boldsymbol{Q}(u)$ commutes with $\boldsymbol{Q}(u')$ and $\boldsymbol{V}(u'')$ for all complex numbers u, u' and u'', the matrix equation (3.2) gives

$$\begin{aligned} V(u)Q(u) &= \phi(u-\lambda)Q(u+2\lambda') + \phi(u+\lambda)Q(u-2\lambda') \\ &= \phi(u+\lambda)Q(u-2\lambda')[1+P(u)] \end{aligned} \tag{3.4}$$

with

$$P(u) = \phi(u-\lambda)Q(u+2\lambda')/\phi(u+\lambda)Q(u-2\lambda') \tag{3.5}$$

where the eigenvalues of $\boldsymbol{V}(u)$ are denoted by $V(u)$, and the corresponding ones of $\boldsymbol{Q}(u)$ by $Q(u)$.

Two further matrices $\boldsymbol{O}$ and $\boldsymbol{R}$ are introduced; $\boldsymbol{O}$ is a diagonal matrix with entries +1 (respectively -1) for arrow configurations of an even (respectively odd) number of down arrows; multiplication by $\boldsymbol{R}$ has the effect of reversing all arrows. It follows that $\boldsymbol{O}$, $\boldsymbol{R}$, $\boldsymbol{Q}(u)$ and $\boldsymbol{V}(u')$ commute with each other for all complex numbers u and u'; the eigenvalues of $\boldsymbol{O}$ (respectively $\boldsymbol{R}$) are denoted by O (respectively R).

We find that the eigenvalue $Q(u)$ must be factorized in the form

$$Q(u) = \exp(tu) \prod_{j=1}^{2N+N'} h[(u-u_j)/2]. \tag{3.6}$$

The zeros u_j and a constant t are determined by the condition that the right-hand side of (3.4) vanishes

$$\begin{aligned} &\left\{ \frac{h^2[(u_j-\lambda)/2]}{h^2[(u_j+\lambda)/2]} \frac{h[(u_j+v'-2\lambda)/2]}{h[(u_j+v')/2]} \frac{h[(u_j+v'-v-\lambda)/2]}{h[(u_j+v'-v+\lambda)/2]} \right\}^N \\ &\qquad \times \left\{ \frac{h[(u_j+v'\mp\lambda-\lambda)/2]}{h[(u_j+v'\mp\lambda+\lambda)/2]} \frac{h[(u_j+v''\mp\lambda-\lambda)/2]}{h[(u_j+v''\mp\lambda+\lambda)/2]} \right\}^{N'} \\ &\quad = -\exp(-4t\lambda') \prod_{k=1}^{2N+N'} \frac{h[(u_j-u_k-2\lambda)/2]}{h[(u_j-u_k+2\lambda)/2]}, \qquad j = 1, 2, \ldots, 2N+N' \end{aligned} \tag{3.7}$$

and the sum rules

$$\begin{aligned} &u_1 + u_2 + \cdots + u_{2N+N'} + (2v' - v - \lambda)N/2 + (v' + v'' \mp 2\lambda)N'/2 \\ &\qquad = (O - 1 + 4N + 2N')I'/2 + \mathrm{i}(OR - 1 + 4N + 2N')I + 2p'I' + 4p\mathrm{i}I \end{aligned} \tag{3.8a}$$

$$t = (O - 1 + 4N + 2N' + 4p')\pi/8I \tag{3.8b}$$

where p and p' are integers. We can find explicit forms of the eigenvalues $V(u)$ by solving (3.7) with (3.8), and then by using (3.6) in (3.4) with solutions u_j and t.

After the eigenvalues $V(u)$ are determined, we can calculate the partition functions in section 2 as

$$Z^{(m)}_{MNN'} = \mathrm{Tr}[\boldsymbol{T}^M \boldsymbol{R}^m] = \sum_j T_j^M R_j^m \tag{3.9}$$

with

$$\boldsymbol{T} = \boldsymbol{V}(-v')\boldsymbol{V}(-v'') \tag{3.10a}$$

$$T_j = V_j(-v')V_j(-v'') \tag{3.10b}$$

where T_j (respectively $V_j(u)$) is the jth eigenvalue of $\boldsymbol{T}$ (respectively $\boldsymbol{V}(u)$) in decreasing order of magnitude; $\boldsymbol{R}$ is inserted to impose two different boundary conditions along the vertical direction: periodic boundary conditions for $m \equiv 0 \pmod 2$ and antiperiodic boundary conditions for $m \equiv 1 \pmod 2$. Using (3.9) and (3.10) in (2.14), we can find the anisotropic interfacial tension of the KEVM.

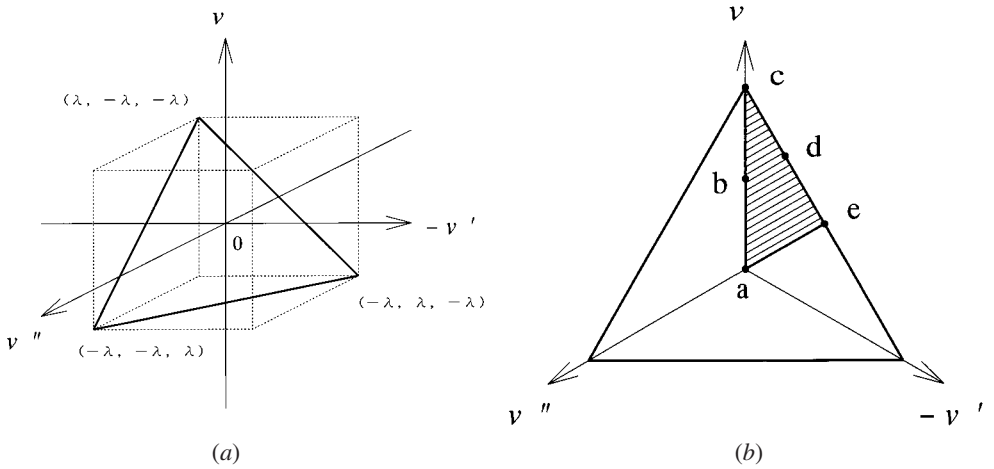

Figure 4. (*a*) The antiferroelectric ordered regime defined by (2.9) and (2.12) is shown in the $(v, -v', v'')$ plane. (*b*) Firstly, we consider the case (3.11), which is indicated by hatched area. Then, using transformations of C_{3v}, we extend the calculation into the antiferroelectric ordered regime. For the five points a–e we draw the ECSs in figure 6.

3.2. Anisotropic interfacial tension

We investigate (3.4)–(3.8) to find the eigenvalues $V(u)$. It is sufficient to consider the case

$$v \geqslant -v' \geqslant v'' \tag{3.11}$$

(figure 4). With the help of transformations of the group C_{3v} [21], we can extend the calculation into the antiferroelectric ordered regime given by (2.9) and (2.12). Firstly, the inhomogeneous system (A) is analysed, and then the inhomogeneous system (B). For each inhomogeneous system it is shown that a doublet of largest eigenvalues are asymptotically degenerate as $N \to \infty$ (with $\eta = N'/N$ fixed to be constant). The anisotropic interfacial tension is derived from finite-size correction terms in this limit.

To analyse the inhomogeneous system (A), we choose the upper signs in (3.3), (3.7) and (3.8). Noting that $V(u)$ is a continuous function of v'', we introduce a real positive number ϵ: $g(u)$ in the last line of (3.1*a*) is redefined as $g(u) = u + v'' - \lambda + \epsilon$; and the related parts in (3.3), (3.7) and (3.8) are modified. Two antiferroelectric ordered states are degenerate in $-v''-\epsilon < \mathrm{Re}\,(u) < -v''$. It is expected that a doublet of largest eigenvalues are asymptotically degenerate in this region. To find the doublet of largest eigenvalues, we repeat almost the same argument in section 3 of [16]; see also [2, 22].

As a beginning, we consider the zero-temperature limit: $k \to 0$ and $I', \lambda, v, v', v'', \epsilon \to \infty$ limit with the ratios $\lambda/I', v/I', v'/I', v''/I', \epsilon/I'$ being order of unity [2, 16, 22]. For the zeros in (3.6) we assume that

$$-v'' - \epsilon < \mathrm{Re}\,(u_j) < -v''. \tag{3.12}$$

Then, (3.7) and (3.8) shows that

$$t = 0 \qquad O = (-1)^{2N+N\eta} \tag{3.13}$$

and that

$$\begin{aligned} u_j \sim -[(2v' - v - \lambda) + \eta(v' + v'' - 2\lambda + \epsilon)]/(4 + 2\eta) + \mathrm{i}2I[2j - (2N + N\eta) \\ -(R + 1)/2]/(2N + N\eta) \qquad j = 1, 2, \ldots, 2N + N\eta \end{aligned} \tag{3.14}$$

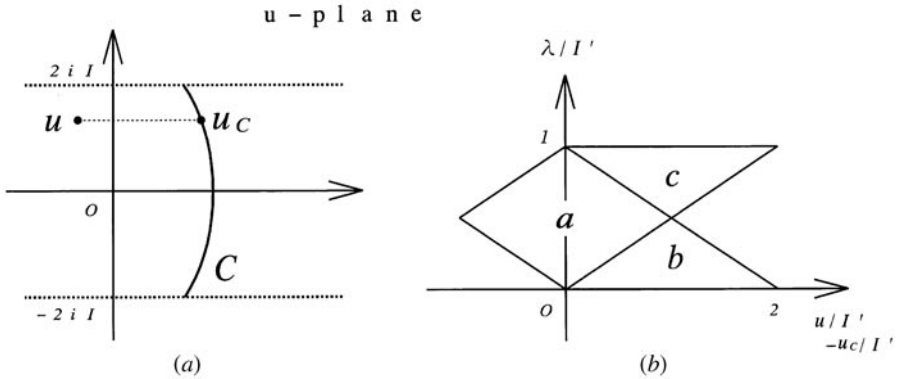

Figure 5. The regions of applicability of (3.17*a*)–(3.17*c*). (*a*) For a given point u, choose a point u_C on the contour C such that Im (u) = Im (u_C). (*b*) Then, using $u - u_C$, we define three regions a, b, and c.

where $R = \pm 1$. The corresponding eigenvalues are denoted by $V_R(u)$. Using (3.13) and (3.14) in (3.4), we obtain for large N

$$\begin{aligned} V_R(u) &\sim R\rho_K^{4N+N\eta}\rho_S^{N\eta}q^{(2N+N\eta)/2}x^{-(4N+2N\eta)}(1-qzy''E/x^2)^{N\eta} \\ &\sim Rc^{2N}(u)c^N(u+v'-\lambda)c^N(u+v'-v)c^{N\eta}(u+v'-\lambda) \\ &\times c^{N\eta}(u+v''-\lambda+\epsilon) \qquad -v' < \mathrm{Re}\,(u) < -v'' \end{aligned} \tag{3.15}$$

where

$$\begin{aligned} x &= \exp(-\pi\lambda/2I) \qquad z = \exp(-\pi u/2I) \\ y'' &= \exp(-\pi v''/2I) \qquad E = \exp(-\pi\epsilon/2I). \end{aligned} \tag{3.16}$$

From (3.15), we identify the two eigenvalues $V_R(u)$ as the doublet of largest eigenvalues. It is noted that in the case (3.11) the condition (3.12) is satisfied when $(3v''-v')/(v-\lambda+\epsilon) < \eta < (3v''-v'+4\epsilon)/(v-\lambda-\epsilon)$.

Here, we return to nonzero temperatures. The zero-temperature results give some useful insights to consider the large-N behaviour. We assume the following properties:

(i) for large N a contour C defined by $|P_R(u)| = 1$ is in the region $-(v'+v''+\epsilon)/2-\lambda <$ Re $(u) < -(v'+v''+\epsilon)/2+\lambda$; the zeros u_j lie on the contour C,

(ii) for a given point u, choose a point u_C on C such that Im (u) = Im (u_C) (figure 5(*a*)); there exists a real positive number δ such that $P_R(u)$ is exponentially larger than 1 as $N \to \infty$ if $-\delta < u - u_C < 0$; $P_R(u)$ is exponentially smaller than 1 if $0 < u - u_C < \delta$,

(iii) $V_R(u)$ is analytic and nonzero in a region which contains C.

Using the properties (i)–(iii), and after some calculations, we find that for large N

$$P_R(u) \sim R\{p^2(u)p(u+v'-\lambda)p(u+v'-v)\}^N\{p(u+v'-\lambda)p(u+v''-\lambda+\epsilon)\}^{N\eta}$$

$$\text{if } |u-u_C| < \min\{2\lambda, 2I'-2\lambda\} \tag{3.17a}$$

$$P_R(u) \sim 1 \qquad \text{if } 2\lambda < u-u_C < 2I'-2\lambda \tag{3.17b}$$

$$\begin{aligned} P_R(u) &\sim \{p^2(u)p(u+v'-\lambda)p(u+v'-v) \\ &\times p^2(u-2I')p(u+v'-\lambda-2I')p(u+v'-v-2I')\}^N \\ &\times\{p(u+v'-\lambda)p(u+v''-\lambda+\epsilon) \\ &\times p(u+v'-\lambda-2I')p(u+v''-\lambda-2I'+\epsilon)\}^{N\eta} \end{aligned}$$

$$\text{if } 2I'-2\lambda < u-u_C < 2\lambda \tag{3.17c}$$

(figure 5) and

$$p(v) = (-z)^{1/2} f(xz^{-1}, x^4)/f(xz, x^4)$$
$$f(a,b) = (1-a)\prod_{n=1}^{\infty}(1-ab^n)(1-a^{-1}b^n)(1-b^n). \tag{3.18}$$

(For detailed derivation, see appendix B of [16].) Since $P_R(u+2I') = P_R(u+4\mathrm{i}I) = P_R(u)$, equations (3.17) determine $P_R(u)$ for all u.

It is also found that in the $N \to \infty$ limit

$$V_R(u) \sim R\rho_K^{4N+N\eta}\rho_S^{N\eta}\kappa^2(u)\kappa(u+v'-\lambda)\kappa(u+v'-v)\kappa^{\eta}(u+v'-\lambda)$$
$$\times\kappa^{\eta}(u+v''-\lambda+\epsilon) \qquad -v''-\epsilon < \mathrm{Re}\,(u) < -v'' \tag{3.19}$$

where

$$\kappa(u) = (\gamma/x)^N \prod_{n=0}^{\infty} \frac{A[u+(4n+3)\lambda]A[u+2I'+(4n-1)\lambda]}{A[u+(4n+5)\lambda]A[u+2I'+(4n+1)\lambda]}$$
$$\times \frac{A[(4n+3)\lambda-u]A[(4n-1)\lambda-u+2I']}{A[(4n+5)\lambda-u]A[(4n+1)\lambda-u+2I']} \tag{3.20}$$

with

$$\gamma = q^{1/4}\Theta(0)\prod_{n=1}^{\infty}(1-q^{2n})^2 \qquad A(u) = \prod_{n=0}^{\infty}(1-q^n z)^N. \tag{3.21}$$

The zero-temperature result (3.15) indicates that (3.19) is analytically continued into $-v' < \mathrm{Re}\,(u) < -v''$.

The solutions (3.17)–(3.21) satisfy the three conditions (i)–(iii). Furthermore, taking the zero-temperature limit, and choosing a suitable direction η, we find that (3.17) and (3.19) reproduce (3.14) and (3.15). Substituting (3.19) into (3.10*b*) gives

$$T_R \sim \lim_{\epsilon\to 0} V_R(-v')V_R(-v'') = \rho_K^{6N}\kappa^2(v)\kappa^2(v')\kappa^2(v''). \tag{3.22}$$

The per-site free energy f_K of the KEVM is calculated as

$$f_K/k_BT = \ln\rho_K + [\ln\kappa(v) + \ln\kappa(v') + \ln\kappa(v'')]/3N. \tag{3.23}$$

Equation (3.23) is coincident with the results in [1, 2, 5]. These facts show the correctness of the argument from (3.12) to (3.21).

In (3.19) the doublet of largest eigenvalues $V_R(u)$ are equal in magnitude and opposite in sign. The Perron–Frobenius theorem implies that the two eigenvalues $V_R(u)$ are asymptotically degenerate when N becomes large. We can find the anisotropic interfacial tension from exponentially small corrections as $N \to \infty$ [2, 5, 16].

For $0 < \lambda < I'/2$, the finite size correction terms are calculated as follows: if N is finite, we obtain

$$\ln[-V_+(u)/V_-(u)] = \frac{1}{8\mathrm{i}I}\int_{C^+} \mathrm{d}u' \ln\left[\frac{1+P_+(u')}{1+P_-(u')}\right] D(u-u')$$
$$-\frac{1}{8\mathrm{i}I}\int_{C^-} \mathrm{d}u' \ln\left[\frac{1+1/P_+(u')}{1+1/P_-(u')}\right] D(u-u')$$
$$-v' < \mathrm{Re}\,(u) < -v'' \tag{3.24}$$

where

$$D(u) = 1 + 2\sum_{n=0}^{\infty}(-1)^n\left\{\frac{x^{2n}z^{-1}}{1-x^{2n}z^{-1}} + \frac{x^{2n+2}z}{1-x^{2n+2}z}\right\} \tag{3.25}$$

(appendix B of [16]). We can find a suitable integration path C^+ (respectively C^-) on the right-hand side (respectively left-hand side) of the contour C (figure 5(a)). Equation (3.17a) shows that, for large N, the logarithms in the integrands of (3.24) can be estimated as

$$\ln\left[\frac{1+P_+(u')}{1+P_-(u')}\right] \sim 2\{p^2(u')p(u'+v'-\lambda)p(u'+v'-v)\}^N \times \{p(u'+v'-\lambda)p(u'+v''-\lambda+\epsilon)\}^{N\eta} \tag{3.26a}$$

$$\ln\left[\frac{1+1/P_+(u')}{1+1/P_-(u')}\right] \sim 2\{p^2(u')p(u'+v'-\lambda)p(u'+v'-v)\}^{-N} \times \{p(u'+v'-\lambda)p(u'+v''-\lambda+\epsilon)\}^{-N\eta}. \tag{3.26b}$$

Substitute (3.26) into (3.24), and integrate (3.24) by the method of steepest descent. After taking the $\epsilon \to 0$ limit, we obtain

$$-V_+(u)/V_-(u) \sim 1+\alpha(u)\{p^2(u_s)p(u_s+v'-\lambda)p(u_s+v'-v)\}^N \times \{p(u_s+v'-\lambda)p(u_s+v''-\lambda)\}^{N\eta}+\cdots \tag{3.27}$$

where the saddle point u_s is determined by

$$\cos\theta\frac{p(2u_s+v'')}{p(u_s)p(u_s+v'-v)}\{1-p^2(u_s)p^2(u_s+v'-v)\} + \sin(\theta-\pi/6)\frac{p(2u_s+v'+v''+\lambda)}{p(u_s+v'+\lambda)p(u_s+v''+\lambda)} \times \{1-p^2(u_s+v'+\lambda)p^2(u_s+v''+\lambda)\}=0 \tag{3.28a}$$

with the condition

$$u_s=-(v'+v'')/2+2\lambda+2\mathrm{i}I \qquad \theta=-\pi/2. \tag{3.28b}$$

The function $\alpha(u)$ is represented by $D(u)$ and the derivative of $p(u)$. Its explicit form is not important here. Equation (3.27) shows that the doublet of the largest eigenvalues $V_R(u)$ are asymptotically degenerate as $N\to\infty$.

If $I'/2<\lambda<I'$, there arise cases where (3.17a) cannot be used to estimate the logarithms in (3.24). Even then, equations (3.26) remain correct, which is shown with the help of integral equations for $P_+(u)/P_-(u)$; see equations (3.22) of [16] and appendix D of [22]. The region of applicability of (3.27)–(3.28) is extended into $0<\lambda<I'$.

Use (3.27), (3.28) in (3.9) and (3.10), and substitute the results into (2.14). We find that for $v\geqslant -v'\geqslant v''$ and $-\pi/2<\theta<0$

$$\sigma/k_BT=-\frac{1}{\sqrt{3}}\cos\theta\ln|p(u_s)p(u_s+v'-v)| - \frac{1}{\sqrt{3}}\sin(\theta-\pi/6)\ln|p(u_s+v'+\lambda)p(u_s+v''+\lambda)|. \tag{3.29}$$

Almost the same calculations are repeated for the inhomogeneous system (B). It follows that (3.29) is analytically continued into $-\pi/2<\theta<\pi/2$ with u_s regarded as a function of θ. Transformations of the group C_{3v} are used to extend (3.29) into $-\lambda<v<-v''<\lambda$ (with $v'=v+v''+\lambda$). As a result, we find that (3.29) gives the expression of the anisotropic interfacial tension throughout the antiferroelectric ordered regime defined by (2.9) and (2.12).

3.3. Equilibrium crystal shape

We now draw the ECS of the KEVM in the X–Y plane. We suppose that a droplet of an ordered phase whose volume (or area) is fixed is embedded inside a sea of another ordered phase.

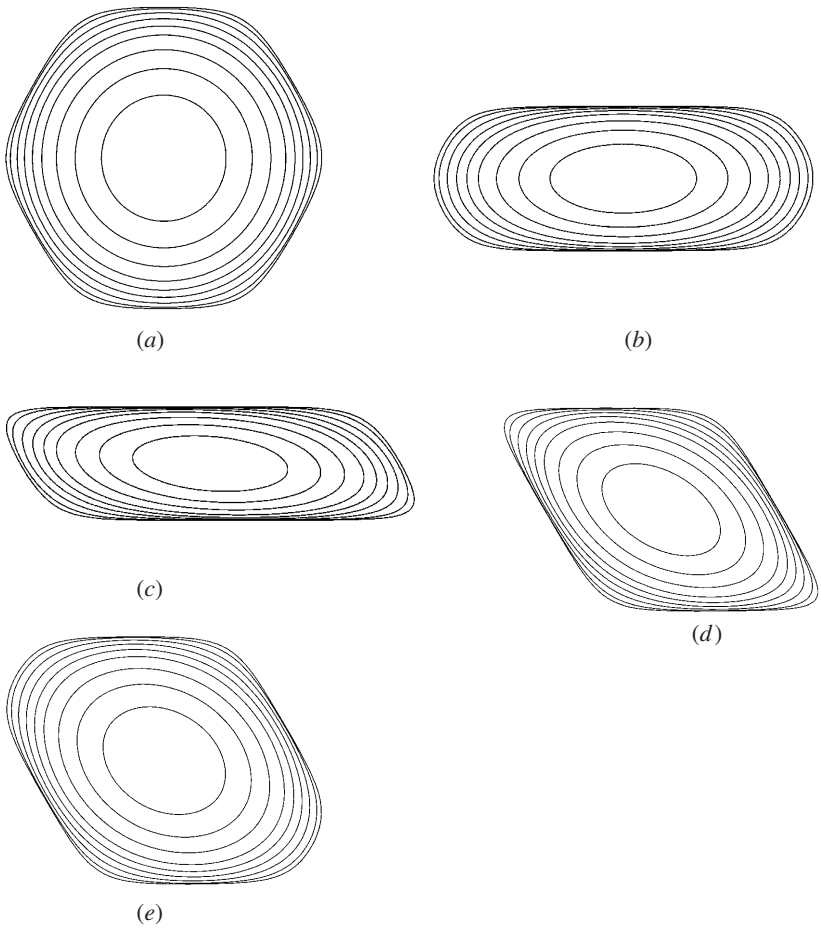

Figure 6. The ECSs of the KEVM given by (3.31)–(3.35) with various values of v, $-v'$, v'': (*a*) the case of isotropic interactions (or $v = -v' = v'' = -\lambda/3$), (*b*) $(v, -v', v'') = (\lambda/3, -2\lambda/3, -2\lambda/3)$, (*c*) $(v, -v', v'') = (\lambda/2, -\lambda/2, -\lambda)$, (*d*) $(v, -v', v'') = (0, 0, -\lambda)$ and (*e*) $(v, -v', v'') = (-\lambda/6, -\lambda/6, -2\lambda/3)$. From the outermost figure, $x = 7.0 \times 10^{-6}$, 1.0×10^{-4}, 0.001, 0.004, 0.01, 0.02, 0.04, 0.07 and 0.12, successively. Each figure is suitably scaled.

The ECS is the droplet shape of the minimum interface free energy obtained from σ via the Wulff construction [9]

$$\Lambda X = \sigma \cos\theta - (\mathrm{d}\sigma/\mathrm{d}\theta)\sin\theta \tag{3.30a}$$

$$\Lambda Y = \sigma \sin\theta + (\mathrm{d}\sigma/\mathrm{d}\theta)\cos\theta \tag{3.30b}$$

where Λ is a scale factor adjusted to yield the volume of the crystal.

Substituting the anisotropic interfacial tension σ calculated in subsection 3.2, and choosing Λ suitably, we obtain

$$\alpha = \exp[-\Lambda(\sqrt{3}X/2 - Y/2)/k_BT] = p(u_s)/p(u_s + v' + \lambda) \tag{3.31a}$$

$$\beta = \exp[-\Lambda Y/k_BT] = p(u_s + v' + \lambda)p(u_s + v'' + \lambda). \tag{3.31b}$$

As u_s moves on the line $\mathrm{Im}\,[u_s] = 2\mathrm{i}I$, (X, Y) sweeps out the ECS (figure 6).

We can rewrite (3.31) into the compact form [5, 8, 12, 14]

$$H_1(\alpha\beta + \alpha^{-1}\beta^{-1}) + H_2(\alpha + \alpha^{-1}) + H_3(\beta + \beta^{-1}) = 1 \tag{3.32}$$

with

$$H_1 = H_0^{-1} \operatorname{snh}[I_1(\lambda - v)/2I] \operatorname{snh}[I_1(\lambda + v')/2I] \tag{3.33a}$$

$$H_2 = H_0^{-1} \operatorname{snh}[I_1(\lambda - v)/2I] \operatorname{snh}[I_1(\lambda - v'')/2I] \tag{3.33b}$$

$$H_3 = H_0^{-1} \operatorname{snh}[I_1(\lambda + v')/2I] \operatorname{snh}[I_1(\lambda - v'')/2I] \tag{3.33c}$$

and

$$H_0 = 2\{\operatorname{dnh}[I_1(\lambda - v'')/2I] \operatorname{dnh}[I_1(\lambda + v')/2I] \times \operatorname{dnh}[I_1(\lambda - v)/2I] + 1\}/k_1^2. \tag{3.34}$$

Definitions of elliptic functions are given in appendix A of [17]; we define the modulus k_1 by requiring that the quarter periods I_1 and I_1' satisfy

$$I_1'/I_1 = \lambda/I. \tag{3.35}$$

4. Summary and discussion

In this paper we investigated the KEVM. We considered the antiferroelectric ordered regime

$$0 < q < x^2 < 1 \qquad x < y''^{-1} < y < x^{-1} \tag{4.1}$$

where q is the nome of the theta functions in (2.1), x and y'' are given by (3.16), and

$$y = \exp(-\pi v/2I). \tag{4.2}$$

The anisotropic interfacial tension σ was calculated by a method which introduces auxiliary vertices into the model. The anisotropic interfacial tension σ is independent of the parameter q. The results in this paper, combined with those in [5], show that in the region $0 < q < x^3$

$$2\sigma/k_B T = 1/\xi \qquad \text{for all directions} \tag{4.3}$$

where ξ is the anisotropic correlation length of the KEVM. The relation (4.3) fails in the region $x^3 < q < x^2$, where ξ depends on the parameter q.

We derived the ECS from σ by applying the Wulff construction. The ECS was given by (3.31)–(3.35). With the help of the homogeneous coordinates, it is shown that (3.32) have two nodes at infinity in the α–β plane (see, for example, [23, 24]). For an algebraic curve of degree m with s nodes and t cusps the genus g is determined by

$$g = (m - 1)(m - 2)/2 - s - t. \tag{4.4}$$

We find that (i) (3.32) represents an elliptic curve (i.e. it is an algebraic curve of genus 1). We calculated σ by expanding (3.24) in the $N \to \infty$ limit. It follows that (ii) the calculation is expressed in terms of differential forms on a Riemann surface of genus 1. The algebraic curve (3.32) is a universal one which appears as the ECSs of various lattice models possessing six-fold rotational symmetry [5, 8, 12, 14]. The property (ii) is applicable to these models.

We reexamine the analysis of ξ in [5], which is helpful to understand physical meanings of the properties (i)–(ii). As shown in (3.30) and (4.3), (3.32) is connected with ξ in the region $0 < q < x^3$. For $x^3 < q < x^2$ it is shown that a similar elliptic curve is related to ξ. Throughout $0 < q < x^2$ calculations of ξ satisfy the property (ii). We note here that (ii) comes from the fact that eigenvalues of the transfer matrix are periodic functions of crystal momentum (which is given by the logarithms of the eigenvalues of the shift operator). It is

also noted that geometry of the elliptic curves is closely related to six-fold rotational symmetry of the model.

For a wide class of lattice models (including unsolvable ones) it is expected that we can choose a suitable Riemann surface of genus 1; and then the property (ii) with spatial symmetries fixes an elliptic curve, which essentially determines the anisotropic correlation length. The eight-vertex model was known as a system where the critical exponents vary continuously as functions of interaction constants [2]; see also [16, 17]. Suzuki [25] proposed the concept of weak universality. The inverse correlation length plays an important role there. We suggest a possibility of interpreting critical phenomena in terms of the moduli space of Riemann surfaces of genus 1 [26,27]. It is more natural to use the modular parameter as a variable measuring the departure from criticality; see (3.31)–(3.35) and [23,24]. Details of this point will be reported in further publications.

References

[1] Baxter R J 1978 *Phil. Trans. R. Soc.* A **289** 315–46
[2] Baxter R J 1982 *Exactly Solved Models in Statistical Mechanics* (London: Academic)
[3] Baxter R J 1986 *Proc. R. Soc.* A **404** 1–33
[4] Baxter R J and Choy T C 1989 *Proc. R. Soc.* A **423** 279–300
[5] Fujimoto M 1998 *J. Stat. Phys.* **90** 363–88
[6] Fujimoto M 1994 *J. Phys. A: Math. Gen.* **27** 5101–19
[7] Fujimoto M 1996 *J. Stat. Phys.* **82** 1519–39
[8] Fujimoto M 1999 *Physica* A **264** 149–70
[9] Wulff G 1901 *Z. Krist. Mineral.* **34** 449–530
Herring C 1951 *Phys. Rev.* **82** 87–93
Burton W K, Cabrera N and Frank F C 1951 *Phil. R. Soc.* A **243** 299–358
[10] van Beijeren H 1977 *Phys. Rev. Lett.* **38** 993–6
Jayaprakash C, Saam W F and Teitel S 1983 *Phys. Rev. Lett.* **50** 2017–20
[11] Rottman C and Wortis M 1981 *Phys. Rev.* B **24** 6274–7
Avron J E, van Beijeren H and Zia R K P 1982 *J. Phys. A: Math. Gen.* **15** L81–6
Zia R K P and Avron J E 1982 *Phys. Rev.* B **25** 2042–5
[12] Zia R K P 1986 *J. Stat. Phys.* **45** 801–13
[13] Holtzer M 1990 *Phys. Rev. Lett.* **64** 653–6
[14] Holtzer M 1990 *Phys. Rev.* B **42** 10 570–82
[15] Akutsu Y and Akutsu N 1990 *Phys. Rev. Lett.* **64** 1189–92
[16] Fujimoto M 1992 *J. Stat. Phys.* **67** 123–54
[17] Fujimoto M 1996 *Physica* A **233** 485–502
[18] Wadati M and Akutsu Y 1988 *Prog. Theor. Phys. Suppl.* **94** 1–41
[19] Wadati M, Deguchi T and Akutsu Y 1989 *Phys. Rep.* **180** 247–332
[20] Suzuki J, Nagao T and Wadati M 1992 *Int. J. Mod. Phys. B* **6** 1119–80
[21] Hammermesh M 1962 *Group Theory and Its Application to Physical Problems* (Reading, MA: Addison-Wesley)
[22] Baxter R J 1973 *J. Stat. Phys.* **8** 25–55
[23] Walker R 1962 *Algebraic Curves* (New York: Dover)
Fulton W 1969 *Algebraic Curves* (New York: Benjamin)
[24] Namba M 1984 *Geometry of Projective Algebraic Curves* (New York: Marcel Dekker)
[25] Suzuki M 1974 *Prog. Theor. Phys.* **51** 1992–3
[26] Fujimoto M 1997 *J. Phys. A: Math. Gen.* **30** 3779–93
[27] Celeghini E, Giachetti R, Sorace E and Tarlini M 1990 *J. Math. Phys.* **31** 2548–50
Bonechi F, Celeghini E, Giachetti R, Sorace E and Tarlini M 1992 *Phys. Rev. Lett.* **68** 3718–20